Article

Mononuclear Aluminum Hydroxide for the Design of Well-Defined Homogeneous Catalysts

Guangcai Bai, Sanjay Singh, Herbert W. Roesky, Mathias Noltemeyer, and Hans-Georg Schmidt

J. Am. Chem. Soc., **2005**, 127 (10), 3449-3455• DOI: 10.1021/ja043585w • Publication Date (Web): 18 February 2005

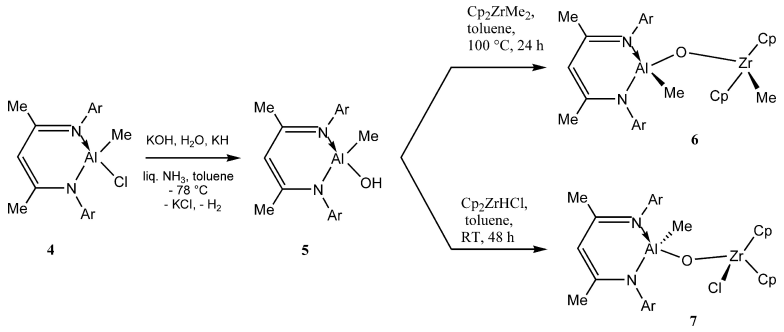

More About This Article

Additional resources and features associated with this article are available within the HTML version:

- Supporting Information
- Links to the 23 articles that cite this article, as of the time of this article download
- Access to high resolution figures
- Links to articles and content related to this article
- Copyright permission to reproduce figures and/or text from this article

View the Full Text HTML

J|A|C|S
ARTICLES
Published on Web 02/18/2005

Mononuclear Aluminum Hydroxide for the Design of Well-Defined Homogeneous Catalysts

Guangcai Bai, Sanjay Singh, Herbert W. Roesky,* Mathias Noltemeyer, and Hans-Georg Schmidt

Contribution from the Institut für Anorganische Chemie der Universität, Göttingen, D-37077 Göttingen, Germany

Received October 22, 2004; E-mail: hroesky@gwdg.de

Abstract: An unprecedented aluminum hydroxide LAlMe(OH) (**5**; L = HC[(CMe)(2,6-*i*Pr$_2$C$_6$H$_3$N)]$_2$) has been prepared by the hydrolysis of LAlMeCl (**4**). For the preparation of **5**, the reagents of KOH, water, and KH, as well as the two-phase ammonia/toluene system, were used. Further reactions of **5** with Cp_2ZrMe_2 (**8**) and Cp_2ZrHCl in toluene lead to the intermolecular elimination of CH_4 and H_2 and the formation of μ-O-bridged dinuclear aluminum and zirconium complexes [LAlMe(μ-O)ZrMeCp$_2$] (**6**) and [LAlMe(μ-O)ZrClCp$_2$] (**7**), respectively, in high yields. The crystal structure reveals that **5** is a monomer with terminal OH and Me groups. The X-ray structure analysis shows that **6** and **7** contain a bent Al−(μ-O)−Zr core with terminal Al−Me and Zr−Me or Zr−Cl arrangements. The methylalumoxane (MAO)-activated compounds **6** and **7** exhibit high catalytic activity for the polymerization of ethylene. Under comparable polymerization conditions, the MAO/**6** and MAO/**7** catalyst systems show considerably higher activity and much lower MAO:catalyst ratios than that of MAO/**8**.

Introduction

The controlled hydrolysis of organoaluminum compounds with water[1] or reactive oxygen-containing species[2] leads to the alkylalumoxanes of general formula $(RAlO)_n$ or $(R_2AlOAlR_2)_n$, which are of tremendous importance for the polymerization of a wide range of organic monomers as highly active catalysts and cocatalysts.[3] Although the trialkylaluminum water adduct $R_3Al{\cdot}H_2O$ and dialkylaluminum hydroxide $R_2Al(OH)$ were proposed to be the intermediates of the controlled hydrolysis of R_3Al based on the variable-temperature ^1H NMR investigations,[4] the isolation of these intermediates is difficult due to their high tendency to form oligomers.[5] Recently, Chen and Chakraborty isolated the first triarylaluminum water complex, $(C_6F_5)_3Al{\cdot}OH_2$, in a controlled reaction of the highly Lewis acidic alane, $(C_6F_5)_3Al$, with water.[6] The isolation and structural characterization of the stable dialkylaluminum hydroxide $R_2Al(OH)$ is a synthetic challenge.

The design and synthesis of single-site homogeneous catalysts for olefin polymerization has developed rapidly in the last few decades.[7] Methylalumoxane (MAO)-containing catalyst systems have been the most extensively studied in both academia and industry since the discovery of MAO as the highly active cocatalyst in ethylene and propylene polymerization by group 4 metallocenes in 1980.[8] Although MAO is the most effective metallocene cocatalyst, the actual molecular structure of the active site remains an open question, and the high MAO:catalyst precursor ratios lead to high cost of the cocatalyst and the high ash content of the polymers. In the course of numerous investigations of the controlled hydrolysis of aluminum compounds, several interesting alumoxanes have been isolated and structurally characterized.[9] However, none of these was as effective as MAO as cocatalyst in the metallocene-catalyzed polymerization of olefins. The design and synthesis of new

(1) (a) Storr, A.; Jones, K.; Laubengayer, A. W. *J. Am. Chem. Soc.* **1968**, *90*, 3173−3177. (b) Ziegler, K. *Angew. Chem.* **1956**, *68*, 721−729. (c) Boleslawski, M.; Pasynkiewicz, S.; Minorska, A.; Hryniów, W. *J. Organomet. Chem.* **1974**, *65*, 165−167.
(2) (a) Kosinska, W.; Kunicki, A.; Boleslawski, M.; Pasynkiewicz, S. *J. Organomet. Chem.* **1978**, *161*, 289−297. (b) Ueyama, N.; Araki, T.; Tani, H. *Inorg. Chem.* **1973**, *12*, 2218−2225. (c) Atwood, J. L.; Hrncir, D. C.; Priester, R. D.; Rogers, R. D. *Organometallics* **1983**, *2*, 985−989.
(3) (a) Feng, T. L.; Gurian, P. L.; Healy, M. D.; Barron, A. R. *Inorg. Chem.* **1990**, *29*, 408−411. (b) Harlan, C. J.; Mason, M. R.; Barron, A. R. *Organometallics* **1994**, *13*, 2957−2969. (c) Mason, M. R.; Smith, J. M.; Bott, S. G.; Barron, A. R. *J. Am. Chem. Soc.* **1993**, *115*, 4971−4984. (d) Wehmschulte, R. J.; Grigsby, W. J.; Schiemenz, B.; Bartlett, R. A.; Power, P. P. *Inorg. Chem.* **1996**, *35*, 6694−6702.
(4) (a) Storre, J.; Klemp, A.; Roesky, H. W.; Schmidt, H.-G.; Noltemeyer, M.; Fleischer, R.; Stalke, D. *J. Am. Chem. Soc.* **1996**, *118*, 1380−1386. (b) Boleslawski, M.; Serwatowski, J. *J. Organomet. Chem.* **1983**, *255*, 269−278.
(5) (a) Pasynkiewicz, S. *Polyhedron* **1990**, *9*, 429−453. (b) Sinn, H.; Kaminsky, W.; Vollmer, H.-J.; Woldt, R. *Angew. Chem.* **1980**, *92*, 396−402; *Angew. Chem., Int. Ed. Engl.* **1980**, *19*, 390−392.
(6) Chakraborty, D.; Chen, E. Y.-X. *Organometallics* **2003**, *22*, 207−210.
(7) (a) Baar, C. R.; Levy, C. J.; Min, E. Y.-J.; Henling, L. M.; Day, M. W.; Bercaw, J. E. *J. Am. Chem. Soc.* **2004**, *126*, 8216−8231. (b) Chen, E. Y.-X.; Metz, M. V.; Li, L.; Stern, C. L.; Marks, T. J. *J. Am. Chem. Soc.* **1998**, *120*, 6287−6305. (c) Brintzinger, H.-H.; Fischer, D.; Mülhaupt, R.; Rieger, B.; Waymouth, R. M. *Angew. Chem.* **1995**, *107*, 1255−1283; *Angew. Chem., Int. Ed. Engl.* **1995**, *34*, 1143−1170. (d) Mohring, P. C.; Coville, N. J. *J. Organomet. Chem.* **1994**, *479*, 1−29. (e) Britovsek, G. J. P.; Gibson, V. C.; Wass, D. F. *Angew. Chem.* **1999**, *111*, 448−468; *Angew. Chem., Int. Ed.* **1999**, *38*, 428−447. (f) Jordan, R. F. *J. Mol. Catal.* **1998**, *128*, 1−337. (g) Kaminsky, W. *Metalorganic Catalysts for Synthesis and Polymerization: Recent Results by Ziegler−Natta and Metallocene Investigations*; Springer-Verlag: Berlin, 1999. (h) Kaminsky, W.; Arndt, M. *Adv. Polym. Sci.* **1997**, *127*, 144−187. (i) Bochmann, M. *J. Chem. Soc., Dalton Trans.* **1996**, 255−270. (j) Marks, T. J. *Acc. Chem. Res.* **1992**, *25*, 57−65. (k) Jordan, R. F. *Adv. Organomet. Chem.* **1991**, *32*, 325−387.
(8) (a) Chen, E. Y.-X.; Marks, T. J. *Chem. Rev.* **2000**, *100*, 1391−1434. (b) Roesky, H. W.; Walawalkar, M. G.; Murugavel, R. *Acc. Chem. Res.* **2001**, *34*, 201−211.

Scheme 1 [a]

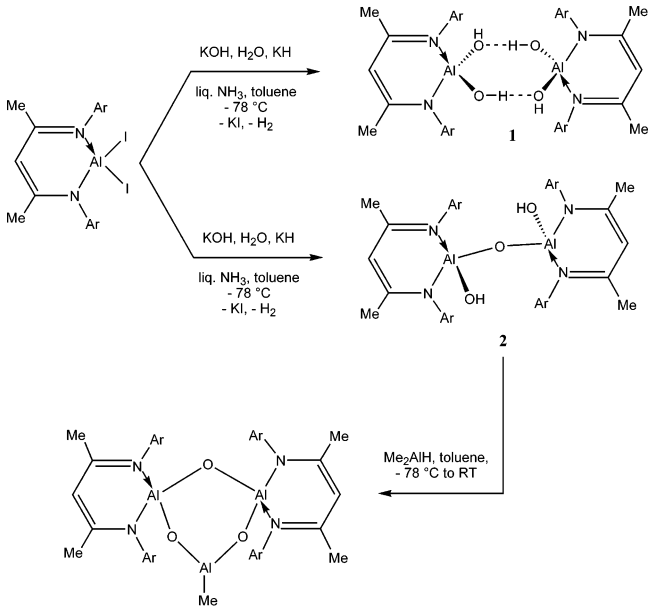

[a] Ar = 2,6-*i*Pr$_2$C$_6$H$_3$.

transition metal catalyst precursors and main-group organometallic cocatalysts is a very important subject, which can provide high catalytic activity with low cocatalyst:catalyst precursor ratio, and allows unprecedented control over the polymer microstructure generating new polymers with improved properties.

Recent work from our laboratory has demonstrated that the liquid ammonia/toluene two-phase system is highly effective for the hydrolysis of organoaluminum compounds. Instead of routine long-chain and three-dimensional cage compounds, we were able to isolate aluminum dihydroxide with terminal OH groups, LAl(OH)$_2$ (**1**; Scheme 1; L = HC[(CMe)(2,6-*i*Pr$_2$-C$_6$H$_3$N)]$_2$),[10] and the first dinuclear alumoxane hydroxide, [LAl-(OH)]$_2$(μ-O) (**2**; Scheme 1), in a two-phase system; the latter compound, when treated with Me$_2$AlH, affords a six-membered alumoxane with a three-coordinate Al center and two-coordinate O atoms, [(LAl)$_2$(MeAl)(μ-O)$_3$][11] (**3**; Scheme 1). Compounds **1** and **2** can be isolated depending on the amount of LAlI$_2$ and KH used. Thus, the reaction of LAlI$_2$ with KOH that contained 10−15% H$_2$O (1:1.3 molar ratio of pure KOH) and KH (1:0.7 molar ratio) results in the formation of **1**, whereas use of LAlI$_2$, KH, and KOH in 1:1.4:0.71 molar ratio leads to the formation of **2**. More recently, we became interested in the preparation of new heterodinuclear aluminum and early transition-metal-containing compounds and the use of such systems as catalysts for the polymerization of olefins.

The previously reported [Cp$_2$ZrMe][(*t*Bu)$_6$Al$_6$(O)$_6$Me] compound synthesized by the reaction of the alumoxane [(*t*Bu)Al-(μ_3-O)]$_6$ with Cp$_2$ZrMe$_2$ (**8**) contains an Al−O−Zr fragment and exhibits catalytic activity for ethylene polymerization.[12] Other hybrid systems, namely, [Al$_7$(μ_3-O)$_6$(*t*Bu)$_6$Me$_3$], show high activity compared to that of the [(*t*Bu)Al(μ_3-O)]$_6$ and MAO systems for the [Me$_2$C(Cp)(Flu)]ZrBz$_2$-catalyzed polymerization of 1,5-hexadiene. In this case, the hybrid alumoxane was prepared by the reaction of trimethyl aluminum and hexameric *tert*-butyl alumoxane.[13] Due to the use of a high amount of MAO, high temperature, and poorly characterized cocatalyst MAO system, effort has been made to develop MAO-free catalyst systems. The search begins with the work of Jordan et al. who discovered the complex, [Cp$_2$ZrMe(THF)]$^+$[BPh$_4$]$^-$.[14a] Several other cationic complexes, for example, [Et(Ind)$_2$Zr(Me)]$^+$-[B(C$_6$F$_5$)$_4$]$^-$ [14b] and {[Cp$_2$ZrMe]$^+$[B(C$_6$F$_5$)$_3$(Me)]$^-$},[14c] are available now which can catalyze olefin polymerization. These systems utilize weakly coordinating anions to stabilize the cation. Roughly comparing the available polymerization data for compound [Cp$_2$ZrMe]$^+$[B(C$_6$F$_5$)$_3$(Me)]$^-$ with the zirconocene/MAO system, we observed that the former exhibits comparable to better catalytic activity. Despite MAO-free and hybrid alumoxane systems, there is still enormous scope for MAO-containing systems in polymerization processes due to higher activity of the latter.

Scheme 2 [a]

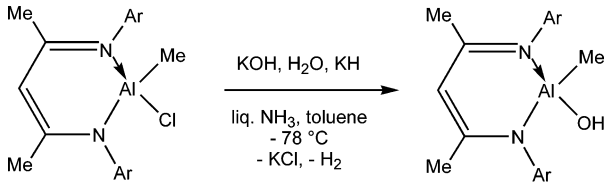

[a] Ar = 2,6-*i*Pr$_2$C$_6$H$_3$.

Herein, we report the synthesis of an unprecedented aluminum hydroxide LAlMe(OH) (**5**) and its reactions with organozirconium compounds for the design of well-defined highly active homogeneous catalysts.

Results and Discussion

Synthesis of LAlMe(OH) (5). Treatment of LAlMeCl (**4**)[15] with KOH containing 10−15% H$_2$O (1:1.3 molar ratio) and KH (1:0.7 molar ratio) in liquid ammonia and toluene at −78 °C results in the complete removal of chloride and the formation of aluminum hydroxide LAlMe(OH) (**5**; Scheme 2). We assume that the initial step of the reaction is the coordination of water to **4**, forming [LMeCl(NH$_3$)$_n$Al·OH$_2$] as an intermediate. Elimination of NH$_4$Cl generates [LMe(NH$_3$)$_{n-1}$Al·(OH)]. The resulting NH$_4$Cl is converted to the less soluble KCl, and the elimination of NH$_3$ from [LMe(NH$_3$)$_{n-1}$Al·(OH)] leads to the formation of **5**. It has been well documented that the hydrolysis of alkylaluminum compounds generates aluminum/water adducts [R$_3$Al·OH$_2$].[4a] A similar mechanism was reported for the

(9) (a) Storre, J.; Schnitter, C.; Roesky, H. W.; Schmidt, H.-G.; Noltemeyer, M.; Fleischer, R.; Stalke, D. *J. Am. Chem. Soc.* **1997**, *119*, 7505−7513. (b) Veith, M.; Jarczyk, M.; Huch, V. *Angew. Chem.* **1998**, *110*, 109−112; *Angew. Chem., Int. Ed.* **1998**, *37*, 105−108. (c) Schmitt, W.; Baissa, E.; Mandel, A.; Anson, C. E.; Powell, A. K. *Angew. Chem.* **2001**, *113*, 3689−3693; *Angew. Chem., Int. Ed.* **2001**, *40*, 3577−3581.
(10) Bai, G.; Peng, Y.; Roesky, H. W.; Li, J.; Schmidt, H.-G.; Noltemeyer, M. *Angew. Chem.* **2003**, *115*, 1164−1167; *Angew. Chem., Int. Ed.* **2003**, *42*, 1132−1135.
(11) Bai, G.; Roesky, H. W.; Li, J.; Noltemeyer, M.; Schmidt, H.-G. *Angew. Chem.* **2003**, *115*, 5660−5664; *Angew. Chem., Int. Ed.* **2003**, *42*, 5502−5506.
(12) Harlan, C. J.; Bott, S. G.; Barron, A. R. *J. Am. Chem. Soc.* **1995**, *117*, 6465−6474.
(13) Watanabi, M.; McMahon, N.; Harlan, C. J.; Barron, A. R. *Organometallics* **2001**, *20*, 460−467.
(14) (a) Jordan, R. F.; Bajgur, C. S.; Willet, R.; Scot, B. *J. Am. Chem. Soc.* **1986**, *108*, 7410−7411. (b) Chien, J. C. W.; Tsai, W.-M.; Rausch, M. D. *J. Am. Chem. Soc.* **1991**, *113*, 8570−8571. (c) Yang, X.; Stern, C. L.; Marks, T. J. *J. Am. Chem. Soc.* **1991**, *113*, 3623−3625.
(15) Compound **4** was prepared by treatment of MeAlCl$_2$ with stoichiometric amounts of LLi in toluene at room temperature in high yield.

Scheme 3 [a]

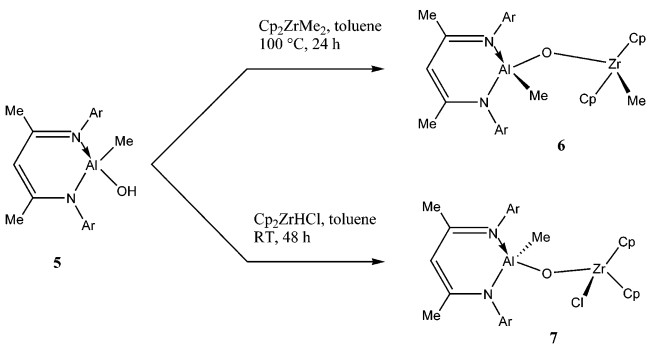

[a] Ar = 2,6-*i*Pr$_2$C$_6$H$_3$.

ammonolysis of aluminum triiodide in the presence of K or KNH_2 in liquid ammonia, which results in the formation of aluminum amides.[16] Meanwhile, **5** could not be isolated from the reaction of LAlMeCl with H_2O in THF or toluene, but results in the complete hydrolysis yielding an insoluble aluminum oxide or hydroxide under elimination of the LH ligand. Obviously, the Lewis acidity of the intermediate [LMe(NH$_3$)$_{n-1}$Al·(OH)] is considerably diminished due to the coordinatively saturated aluminum center with the ammonia donor molecules. In addition, the reaction occurring preferentially at the interface can be rationalized as the two-phase system (ammonia/toluene) which increases the solubility of the inorganic and organic components in the system. Therefore, we believe that the liquid ammonia/toluene two-phase system is essential for the formation of **5**, and the sterically encumbered β-diketiminato ligand on aluminum is stabilizing the monomeric aluminum hydroxide.

Compound **5** is a colorless crystalline solid with the melting point of 192 °C. To our surprise, no decomposition or polymerization was observed when **5** was kept in toluene solution or in the solid state under an inert atmosphere. The most intense peak in the EI mass spectrum of **5** appeared at *m*/*z* 461 [M$^+$ − Me], and the peak at 443 (20%) was assigned to the fragment [M$^+$ − Me − H_2O]. The ^{1}H NMR spectrum of **5** shows two singlets at δ 0.53 and −0.88 ppm which can be attributed to the protons of OH and AlMe groups, respectively.

Synthesis of [LAlMe(μ-O)ZrMeCp$_2$] (6) and [LAlMe(μ-O)ZrClCp$_2$] (7). Further reaction of **5** with 1 equiv of Cp$_2$ZrMe$_2$ (**8**) in toluene at 100 °C leads to intermolecular elimination of CH_4 and the formation of μ-O-bridged heterodinuclear complex [LAlMe(μ-O)ZrMeCp$_2$] (**6**; Scheme 3) in high yield (93%). Similarly, treatment of **5** with stoichiometric amounts of Cp$_2$ZrHCl in toluene at room temperature results in the formation of μ-O-bridged dinuclear aluminum and zirconium compound [LAlMe(μ-O)ZrClCp$_2$] (**7**; Scheme 3) in high yield (89%).

Compounds **6** and **7** are colorless crystalline solids with melting points of 385 and 396 °C, respectively. Decomposition was observed at the melting point of **6** and **7**. The most intense peak in the EI mass spectrum of **6** appears at *m*/*z* 695 [M$^+$ − Me]. Compound **7** exhibits the fragment [M$^+$ − Me] at 715 as the base peak. The ^{1}H NMR spectrum of **6** shows two singlets at δ −0.32 and −0.72 ppm which can be attributed to the Me protons of ZrMe and AlMe groups, respectively, whereas the corresponding AlMe protons in **7** resonate at δ −0.66 ppm.

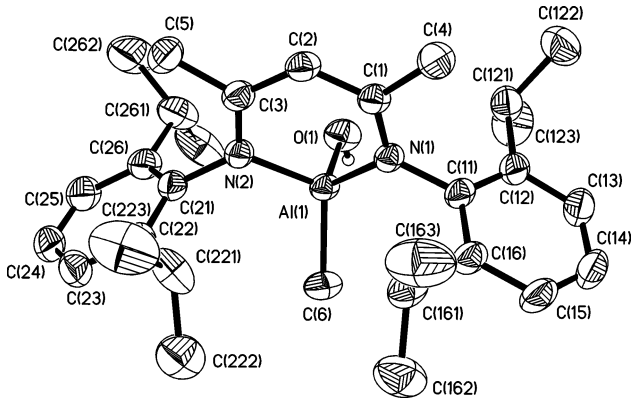

Figure 1. Molecular structure of LAlMe(OH) (**5**) in the crystal (50% probability ellipsoids); only hydrogen atom on −OH group is shown.

Molecular Structure of 5. Single crystals of **5**, suitable for X-ray structural analysis, were obtained by maintaining the reaction mixture in toluene at −20 °C for 1 week. Compound **5** crystallizes in the monoclinic space group *P*2(1)/*c*. The X-ray structure reveals **5** as a monomeric aluminum hydroxide (Figure 1). The Al center exhibits a distorted tetrahedral geometry with two nitrogen atoms of the β-diketiminato ligand, one Me, and an OH group. The small N−Al−N angle (96.3(1)°) is the result of formation of the C_3N_2Al six-membered ring. The Al−OH bond length (1.731(3) Å) is slightly longer than those found in **1** (1.695(15) and 1.711(16) Å)[10] and comparable to those in **2** (1.738(3) and 1.741(3) Å),[11] but significantly shorter than those of Al−(μ-OH) bonds in [(Ph$_2$Si)$_2$O$_3$]$_4$Al$_4$(μ-OH)$_4$ (∼1.800 Å),[17] [Mes$_2$Al(μ-OH)]$_2$·2THF (1.822(1) Å; Mes = mesityl),[4a] and Al$_5$(tBu)$_5$(μ_3-O)$_2$(μ_3-OH)$_2$(μ-OH)$_2$(μ-O$_2$CPh)$_2$ (∼1.824 Å).[18] The Al−Me bond length (1.961(3) Å) is comparable to those found in Al(Me)(mqp)$_2$ (1.964(6)Å; mqp = 2-(4′-methylquinolinyl)-2-phenolato)[20] and (OCMeCHCMeNAr)$_2$AlMe (1.975(2) Å).[21]

Molecular Structures of 6 and 7. The molecular structures of **6** and **7** are shown in Figures 2 and 3, respectively. Compound **6** crystallizes in the triclinic space group $P\bar{1}$ and **7** in orthorhombic space group *Pnma*. Compounds **6** and **7** contain a bent Al−O−Zr core. The Al atom exhibits a highly distorted tetrahedral geometry with two nitrogen atoms of the ligand, a Me group, and one (μ-O) unit. The coordination sphere of zirconium is completed by two Cp ligands and one Me group (in **6**) and Cl atom (in **7**). The Me groups on Al and Zr in **6** are bent out of the Al−O−Zr plane in a cis manner, whereas in **7**, the Me group on Al and the Cl atom on Zr are trans to each other with respect to the Al−O−Zr moiety.

The Al−(μ-O) bond length (1.711(2) Å) is longer than those found in compounds **2** (1.698(3) and 1.694(3) Å), [{(Me$_3$Si)$_2$HC}$_2$Al]$_2$(μ-O) (1.687(4) Å),[22] and [HC{(CMe)(NMe)}$_2$AlCl]$_2$(μ-O) (1.677(6) Å).[19] The Al−(μ-O)−Zr angle (158.2(1)°) is wider than the Al−(μ-O)−Al angle in **2** (143.9(2)°), but significantly narrower than the Zr−(μ-O)−Zr angle

(16) (a) Taylor, W. L.; Griswold, E.; Kleinberg, J. *J. Am. Chem. Soc.* **1955**, *77*, 294−298. (b) Watt, G. W.; Hall, J. L.; Choppin, G. R. *J. Phys. Chem.* **1953**, *57*, 567−570.

(17) Veith, M.; Jarczyk, M.; Huch, V. *Angew. Chem.* **1997**, *109*, 140−142; *Angew. Chem., Int. Ed. Engl.* **1997**, *36*, 117−119.
(18) Koide, Y.; Barron, A. R. *Organometallics* **1995**, *14*, 4026−4029.
(19) Kuhn, N.; Fuchs, S.; Niquet, E.; Richter, M.; Steimann, M. *Z. Anorg. Allg. Chem.* **2002**, *628*, 717−718.
(20) Liu, S.-F.; Seward, C.; Aziz, H.; Hu, N.-X.; Popović, Z.; Wang, S. *Organometallics* **2000**, *19*, 5709−5714.
(21) Yu, R.-C.; Hung, C.-H.; Huang, J.-H.; Lee, H.-Y.; Chen, J.-T. *Inorg. Chem.* **2002**, *41*, 6450−6455.
(22) Uhl, W.; Koch, M.; Hiller, W.; Heckel, M. *Angew. Chem.* **1995**, *107*, 1122−1124; *Angew. Chem., Int. Ed. Engl.* **1995**, *34*, 117−119.

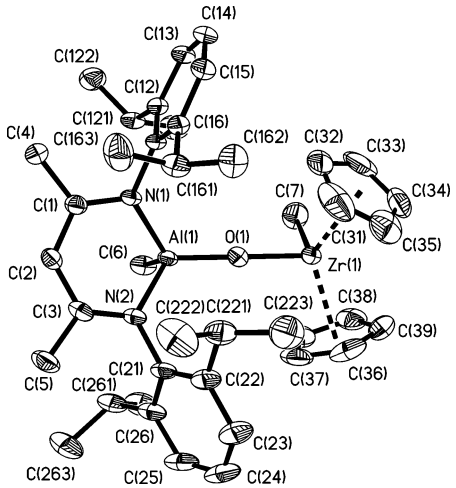

Figure 2. Molecular structure of [(LAlMe)(Cp_2ZrMe)](μ-O) (**6**) in the crystal (50% probability ellipsoids); hydrogen atoms are omitted for clarity.

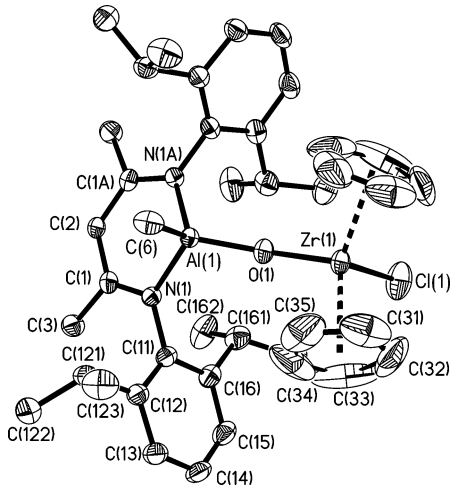

Figure 3. Molecular structure of [(LAlMe)(Cp_2ZrCl)](μ-O) (**7**) in the crystal (50% probability ellipsoids); hydrogen atoms are omitted for clarity.

in compound (Cp_2ZrMe)$_2$(μ-O) (174.1(3)°).[23] The Al−Me bond length (1.961(3) Å) is similar to that of **5**.

The Zr−(μ-O) bond length (1.929(2) Å) is slightly shorter than those exhibited by compounds [(Cp_2ZrCl)$_2$(μ-O)] (1.945(3) Å),[24] (Cp_2ZrMe)$_2$(μ-O) (1.948(1) Å),[23] and [{Cp_2Zr-(μ-O)}$_3$] (1.959(3) Å),[25] but significantly shorter than the Zr−(μ-O) or Zr−(μ-OH) bond lengths observed in clusters [(Cp^*Zr)$_6$-(μ_4-O)(μ-O)$_4$(μ-OH)$_8$]·2(C_7H_8) (∼2.106 Å)[26] and [{(Cp^*ZrCl)(μ-OH)}$_3$(μ_3-OH)(μ_3-O)]·2THF (2.160(2) Å).[27] The Zr−Me bond length (2.286(3) Å) is comparable to those found in compound (Cp_2ZrMe)$_2$(μ-O) (2.276(9) Å).[23]

The Al−(μ-O) (1.727(3) Å) and the Al−Me (1.959(3) Å) bond lengths as well as the Al−(μ-O)−Zr angle (155.4(1)°) in **7** are comparable to those observed in **6**. The Zr−Cl bond length (2.463(3) Å) is comparable to those found in [Zr{Me_2C(η-C_5H_4)$_2$}Cl]$_2$(μ-O) (2.466(2) and 2.467(2) Å).[28]

OH Functional Group of 5. The OH groups are the most important functional groups for solid support as well as for the immobilization of catalytically active metal complexes and also for solid acid catalysts.

The IR spectrum (Nujol) of **5** exhibits a sharp band (3728 cm^{-1}) for the terminal OH group, which is in agreement with the solid-state structure of **5**. The absorption frequency of the OH group in **5** is comparable to that of the terminal OH groups found in compounds **1** (3727 cm^{-1}) and **2** (3716 cm^{-1}), but higher than those found in the Brönsted acids, SAPO-34 (3600−3625 cm^{-1})[29] and zeolite Chabazite (3603 cm^{-1}).[30] Therefore, **5** contains a free Brönsted acidic OH group. The acidity of **5** can be anticipated due to the Lewis acidic Al(III) center and high bond strength of the Al−O bond. Furthermore, in the ^{1}H NMR spectrum, the proton of the OH group in **5** resonates at δ 0.53 ppm. This result is similar to that observed for **2** (δ −0.30 ppm). It is noteworthy that on one hand the OH group of **5** is reactive enough to react with Cp_2ZrMe_2 and Cp_2ZrHCl to yield **6** and **7** as described, as well as with AlH_3·NMe_3 and GaH_3·NMe_3,[31] on the other, it does not impede the formation of **5** during the course of the reaction as it does not eliminate methane, presumably kinetic stability disfavors intermolecular methane evolution due to the sterically encumbered β-diketiminato ligand.

Polymerization of Ethylene with [LAlMe(μ-O)$ZrMeCp_2$] (6) and with [LAlMe(μ-O)$ZrClCp_2$] (7): A Comparison with Cp_2ZrMe_2 (8). When activated with MAO, **6** and **7** catalyze the polymerization of ethylene in toluene. All of the polymeric materials were isolated as white powders. To compare the catalytic activity of **6** and **7** with that of Cp_2ZrMe_2 (**8**), the polymerizations of ethylene using MAO/**8** as a catalyst were performed under conditions similar to those for MAO/**6** or MAO/**7**.

A. TOF Values of 6, 7, and 8. Table 3 summarizes the TOF values of catalysts **6**, **7**, and **8**, and Figure 4 shows the plot of TOF values for different ratios of MAO:**6** and different ratios of MAO:**8**. Under the same conditions, such as concentration of catalyst (2×10^{-4} M toluene solution of catalyst) and amount of MAO (MAO:catalyst 136:1; 610, 704, and 804), the TOF value of **6** (1.03×10^6 g PE/mol cat·h) is higher than that of **7** (8.4×10^5 g PE/mol cat·h), but significantly higher than that of Cp_2ZrMe_2 (8.0×10^4 g PE/mol cat·h). Figure 4 illustrates that the TOF values of **6** are significantly improved with the increase of the MAO in the range from 32 to 150, which can further be slightly improved at higher ratios (>150). Under our experimental conditions, the optimized ratio of MAO:**6** is in the range of 100:1 to 200:1 with the TOF values ranging from 1.0 to 1.2 $\times 10^6$ g PE/mol cat·h.

B. Polymerization Rates of 6 and Cp_2ZrMe_2 (8). Table 4 gives the reaction rates r at time t, and Figure 5 illustrates the plot of reaction rate r to time t for **6** and for **8**. It can be clearly seen that the polymerization rates increase faster, and that the highest r value is maintained for relatively longer time for **6**

(23) Hunter, W. E.; Hrncir, D. C.; Vann Bynum, R.; Penttila, R. A.; Atwood, J. L. *Organometallics* **1983**, *2*, 750−755.
(24) Clarke, J. F.; Drew, M. G. B. *Acta Crystallogr.* **1974**, *B30*, 2267−2269.
(25) Fachinetti, G.; Floriani, C.; Chiesi-Villa, A.; Guastini, C. *J. Am. Chem. Soc.* **1979**, *101*, 1767−1775.
(26) Bai, G.; Roesky, H. W.; Li, J.; Labahn, T.; Cimpoesu, F.; Magull, J. *Organometallics* **2003**, *22*, 3034−3038.
(27) Babcock, L. M.; Day, V. W.; Klemperer, W. G. *J. Chem. Soc., Chem. Commun.* **1988**, 519−520.
(28) Green, J. C.; Green, M. L. H.; Taylor, G. C.; Saunders, J. *J. Chem. Soc., Dalton Trans.* **2000**, 317−327.
(29) Shah, R.; Gale, J. D.; Payne, M. C. *Chem. Commun.* **1997**, 131−132.
(30) Ugliengo, P.; Civalleri, B.; Zicovich-Wilson, C. M.; Dovesi, R. *Chem. Phys. Lett.* **2000**, *318*, 247−255.
(31) Singh, S.; Kumar, S. S.; Chandrasekhar, V.; Ahn, H.-J.; Biadene, M.; Roesky, H. W.; Hosmane, N. S.; Noltemeyer, M.; Schmidt, H.-G. *Angew. Chem.* **2004**, *116*, 5048−5051; *Angew. Chem., Int. Ed.* **2004**, *43*, 4940−4943.

Table 1. Crystallographic Data for **5**, **6**, and **7**

	5	**6**	**7**
empirical formula	$C_{30}H_{45}AlN_2O$	$C_{41}H_{57}AlN_2OZr$	$C_{40}H_{54}AlClN_2OZr$
formula weight	476.66	712.09	732.50
color	colorless	colorless	colorless
crystal system	monoclinic	triclinic	orthorhombic
space group	$P2(1)/c$	$P\bar{1}$	*Pnma*
a, Å	9.036(3)	9.968(5)	18.375(2)
b, Å	9.763(4)	10.314(8)	20.171(4)
c, Å	33.17(6)	19.684(16)	10.0747(9)
α, deg	90	87.99(7)	90
β, deg	91.40(6)	87.06(4)	90
γ, deg	90	68.49(5)	90
V, Å^3	2926(6)	1880(2)	3734.1(9)
Z	4	2	4
ρ_{calc}, g cm^{-3}	1.082	1.258	1.303
μ, mm^{-1}	0.092	0.349	0.422
F (000)	1040	756	1544
2θ range, deg	7.10−50.12	7.14−50.08	7.24−50.00
No. of collected reflns	6159	6325	5395
No. of unique reflns	4899 (R_{int} = 0.1157)	5932 (R_{int} = 0.0507)	3368 (R_{int} = 0.0708)
data/restraints/params	4899/0/322	5932/0/427	3368/0/223
refinement method	full-matrix least-squares on F^2	full-matrix least-squares on F^2	full-matrix least-squares on F^2
R^a, $wR2^b$ ($I > 2\sigma(I)$)	0.0755, 0.2231	0.0430, 0.1153	0.0364, 0.0945
R, *wR*2 (all data)	0.0846, 0.2303	0.0446, 0.1171	0.0404, 0.0987
goodness of fit, S^c	1.058	1.093	1.061
largest diff peak, hole (e Å^{-3})	+0.551/−0.410	+0.777/−1.1148	+0.495/−0.859

[a] $R = \sum||F_o| - |F_c||/\sum|F_o|$. [b] $wR2 = [\sum w(F_o^2 - F_c^2)^2/\sum w(F_o^2)]^{1/2}$. [c] $S = [\sum w(F_o^2 - F_c^2)^2/\sum(n - p)]^{1/2}$.

Table 2. Selected Bond Lengths (Å) and Bond Angles (deg) for LAlMe(OH) (**5**), [LAlMe(*μ*-O)ZrMeCp$_2$] (**6**), and [LAlMe(*μ*-O)ZrClCp$_2$] (**7**)

	5	**6**	**7**
	Bond Lengths		
Al(1)−O(1)	1.731(3)	1.711(2)	1.727(3)
Al(1)−N(1)	1.904(3)	1.910(3)	1.909(2)
Al(1)−N(2)[a]	1.907(3)	1.929(3)	1.909(2)
Al(1)−C(6)	1.961(3)	1.961(3)	1.959(3)
Zr(1)−O(1)		1.929(2)	1.920(3)
Zr(1)−C(7)		2.286(3)	
Zr(1)−Cl(1)			2.463(3)
Zr(1)−centroid Cp		2.254(2)	2.246(3)
	Bond Angles		
O(1)−Al(1)−N(1)	105.8(1)	113.9(1)	111.5(4)
O(1)−Al(1)−N(2)[a]	108.1(1)	112.0 (1)	111.5(8)
N(1)−Al(1)−N(2)[a]	96.3(1)	95.2(1)	97.3 (1)
O(1)−Al(1)−C(6)	116.6(2)	113.2 (1)	114.3(2)
N(1)−Al(1)−C(6)	115.0(1)	111.6(1)	110.5(1)
N(2)[a]−Al(1)−C(6)	113.0(2)	109.5(1)	110.5(1)
Al(1)−O(1)−Zr(1)		158.2(1)	155.4(1)
O(1)−Zr(1)−C(7)		100.2(1)	
O(1)−Zr(1)−Cl(1)			102.0(7)

[a] N(2) corresponds to N(1A) for **7**.

Table 3. TOF (g PE/mol cat·h × 10^{-6}) Values of **6**, **7**, and **8**

catalysts[a]	MAO:catalyst	*t* (min)	PE (g)	TOF	$10^{-3}\times M_w$	M_w/M_n
601	32	60	0.89	0.05		
602	48	60	7.8	0.39	194.86	10.76
603	96	30	9.0	0.90	80.23	10.00
604	136	30	10.9	1.09	62.68	8.13
605	176	30	11.9	1.19		
606	272	30	12.4	1.24		
607	400	30	12.7	1.27		
608	176	30	9.9	1.32		
609	176	120	7.6	0.39	306.11	10.13
610	136	18	6.2	1.03	86.96	12.28
611	272	30	10.9	1.09		
704	136	30	8.4	0.84	108.67	21.47
705	176	30	11.4	1.14		
804	136	120	3.3	0.08	471.94	5.58
805	176	73	12.8	0.52	165.25	16.34
806	272	60	14.6	0.73		
807	400	37	14.8	1.20		

[a] 601−607, 610, and 611, 2.0 × 10^{-4} M toluene solution of **6**; 608, 1.5 × 10^{-4} M toluene solution of **6**; 609, 1.0 × 10^{-4} M toluene solution of **6**; 704 and 705, 2 × 10^{-4} M toluene solution of **7**; 804−807, 2 × 10^{-4} M toluene solution of Cp_2ZrMe_2 (**8**).

compared to **8**. The higher the MAO:catalyst ratio is, the faster the highest rate is achieved and sustained for a longer period. Even at the highest MAO:catalyst ratio (400), for **8**, the reaction rate attains the highest value in more than 10 min and sustains this value for a very short time (about 2 min). It is interesting to compare the reaction rates of **6** at low MAO:catalyst ratio (48:1; 602) with those of **8** at much higher MAO:catalyst ratio (176:1; 805). Figure 6 shows that the reaction rates of **6** at low MAO:catalyst ratio increase slowly and attain their highest value (0.52) after 55 min and maintain this value at least for 60 min (we had to stop the reaction after 1 h due to the high content of solid in the flask). In comparison, the reaction rates of **8** increase faster at the beginning, reach their highest value (0.33) after 41 min, and decrease after 50 min. Therefore, even at low MAO:catalyst ratio, **6** exhibits much higher reactivity and longer lifetime compared to **8**. These features were not observed even with relatively high MAO:catalyst ratio with the latter.

C. Influence of the Reaction Time of 6 with MAO to the TOF Values. For 601−607, MAO (0.2 mL, 0.32 mmol of Al) was added to the toluene solution (100 mL) containing 20 *μ*mol of **6**. After 20 min (no polymerization was observed in the initial 20 min), the rest of MAO was added and the polymerization started. Table 3 shows that the TOF values for preactivated **6** (604, 1.09 × 10^6 g PE/mol cat·h, MAO:**6** = 176:1; 606, 1.24 × 10^6 g PE/mol cat·h, MAO:**6** = 272:1) are slightly higher than those without preactivated **6** under the same conditions (610, 1.03 × 10^6 g PE/mol cat·h, MAO:**6** = 176:1; 611, 1.09

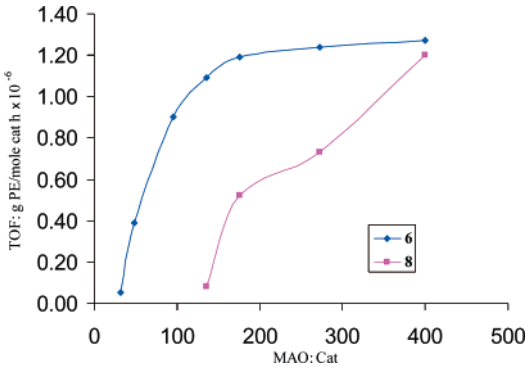

Figure 4. Plot of TOF values versus MAO:catalyst ratios of **6** and Cp_2ZrMe_2.

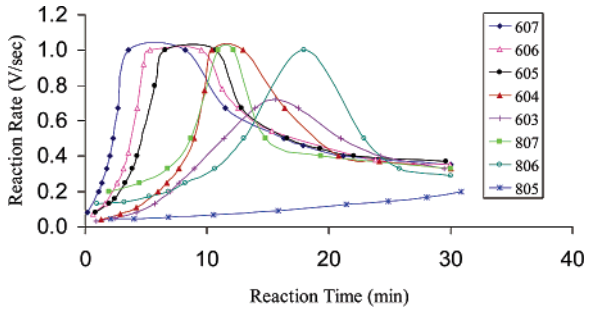

Figure 5. Plot of reaction rate versus time of **6** and Cp_2ZrMe_2 (**8**).

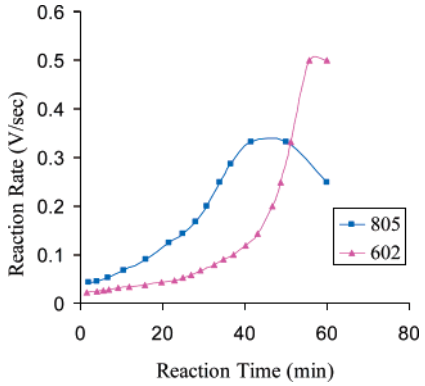

Figure 6. Plot of reaction rate versus time of **6** (MAO:catalyst = 48) and Cp_2ZrMe_2 (**8**) (MAO:catalyst = 176).

$\times$ 10^6 g PE/mol cat·h, MAO:**6** = 272:1). Meanwhile, when MAO (0.2 mL, 0.32 mmol of Al) was added to the toluene solution (100 mL) containing 20 μmol of Cp_2ZrMe_2 (**8**), the solution became cloudy after 20 min. We assume that the addition of small amounts of MAO at the initial stage enhances the formation of the catalytically active center of **6**, and the polymer yields are better with preactivated catalyst.

D. Influence of the Concentration of 6 to the TOF Values. To investigate the influence of the concentration of **6** to the TOF values, different concentrations of **6** (605, 2.0×10^{-4} M; 608, 1.5×10^{-4} M; 609, 1.0×10^{-4} M) under the same MAO:catalyst ratio (176:1) were used. It is interesting to observe (Table 3) that the TOF value of **6** in a 1.5×10^{-4} M toluene solution (1.32×10^6 g PE/mol cat·h) is higher than that in a 2.0×10^{-4} M solution (1.19×10^6 g PE/mol cat·h), but significantly higher than that in a 1.0×10^{-4} M solution (0.39×10^6 g PE/mol cat·h). This indicates that the TOF values are greatly influenced by the catalyst concentration.

The exact mechanism for the formation of the catalytically active species involved is not established; it is possible that at initial stages, MAO abstracts the Me group from zirconium-yielding cationic zirconium species which is subsequently stabilized by transfer of the methyl group from Al to Zr. It has been demonstrated that when the Al:Zr ratio is increased from a few hundreds to thousands, the **8**/MAO system becomes catalytically active, and excess of MAO serves to abstract a Me group from Cp_2ZrMe_2 (**8**) and, at the same time, acts as a scavenger for O_2, H_2O, and other protic impurities in the system. If the role of MAO is only to abstract Me and to clean up the system, the reactivity of Cp_2ZrMe_2 (**8**) should be much higher than that of **6**. The in situ formation of a stable catalytically active center greatly decreases the MAO:Zr ratio. Therefore, we assume that some of the O centers in MAO coordinate further to stabilize the Zr center of **6**.

Conclusions

In this part of the study, a new synthetic approach for the hydrolysis of aluminum compounds is presented, involving a liquid NH_3/toluene two-phase system, yielding hitherto unknown LAlMe(OH) species. To the best of our knowledge, compound **5** represents an unprecedented monomeric aluminum hydroxide. Isolation of **5** enables us to obtain structural details on extremely unstable intermediates from the hydrolysis reaction of R_3Al. The Brönsted acidic OH group of **5** reacts with organometallic compounds containing relatively basic fragments to give rise to well-characterized lipophilic heterobimetallic compounds[31] with an Al(μ-O)M core, such as **6** and **7**. This methodology

Table 4. Polymerization Rates, *r* (V/sec), at Time, *t* (min), of **6** and Cp_2ZrMe_2

603		604		605		606		607		805		806		807	
t	*r*	*t*	*r*	*t*	*r*	*t*	*r*	*t*	*r*	*t*	*r*	*t*	*r*	*t*	*r*
0.96	0.03	1.33	0.04	0.85	0.08	0.68	0.07	0.20	0.08	2.10	0.043	0.98	0.13	1.97	0.20
2.52	0.05	2.92	0.07	1.98	0.13	1.62	0.13	1.10	0.20	4.00	0.045	3.23	0.14	4.50	0.25
4.21	0.08	4.23	0.11	2.42	0.16	2.60	0.25	1.40	0.25	6.85	0.053	5.25	0.17	6.80	0.33
5.72	0.13	5.96	0.20	3.30	0.25	3.18	0.33	1.75	0.33	10.50	0.067	6.83	0.20	8.70	0.50
6.98	0.20	6.69	0.25	3.90	0.33	3.52	0.42	2.03	0.40	15.85	0.091	8.23	0.25	10.92	1.00
7.67	0.25	7.68	0.33	4.30	0.40	4.30	0.67	2.27	0.50	21.48	0.125	10.63	0.33	12.18	1.00
8.98	0.33	8.95	0.50	5.75	0.80	4.83	0.92	2.72	0.67	24.90	0.143	13.00	0.50	14.80	0.50
11.37	0.50	9.80	0.77	6.60	1.00	5.35	1.00	3.58	1.00	28.00	0.167	17.93	1.00	19.33	0.40
13.92	0.67	10.38	1.00	10.70	1.00	9.56	1.00	8.25	1.00	30.88	0.200	22.88	0.50	30.00	0.33
15.58	0.72	12.97	1.00	12.80	0.67	11.25	0.78	11.50	0.07			25.78	0.33		
17.48	0.67	16.37	0.67	16.58	0.50	12.58	0.67	16.30	0.50			30.00	0.29		
21.00	0.50	20.77	0.40	19.30	0.44	15.30	0.54	17.91	0.46						
24.20	0.40	24.12	0.37	22.01	0.40	23.81	0.38	21.20	0.40						
29.48	0.33	30.00	0.33	29.59	0.37	29.95	0.35	30.00	0.35						

provides incentives to the development of a new and potential area of molecular catalysis in homogeneous systems. Moreover, we have shown that zirconocene derivatives **6** and **7** exhibit high catalytic activity for ethylene polymerization with much lower MAO:catalyst ratios than those of the MAO:Cp_2ZrMe_2 (**8**) catalytic system under similar conditions. This observation suggests that the polymerization activity and the catalyst:MAO ratio can be influenced substantially by the structure of the zirconocene. Moreover, we also speculate that not only the structure of zirconocene is important to determine the activity of **6** and **7** but also the stability of the active species is important, that is, cation−anion interaction and the concentration of the active species are crucial. The latter factor is favored with the **6**/MAO and **7**/MAO compared to the **8**/MAO system. We anticipate that a series of aluminum transition metal catalyst precursors could be generated in a rational and predictable manner, which can provide a highly active catalyst with a low cocatalyst:catalyst precursor ratio and, hopefully, allow unprecedented control over polymer microstructure, generating new polymers with improved properties.

Experimental Section

General Remarks. All manipulations were carried out under an atmosphere of purified nitrogen using standard Schlenk techniques. Samples prepared for spectral measurements as well as for reactions were manipulated in a glovebox. Solvents were dried using conventional procedures, distilled under nitrogen, and degassed prior to use. Deuterated NMR solvents were treated with K/Na alloy, distilled, and stored under nitrogen.

The ^{1}H NMR spectra were recorded on Bruker AM 200 NMR spectrometer with $SiMe_4$ as external standard. Mass spectra were recorded on a Finnigan MAT 8230 mass spectrometer using the EI-MS method. The most intense peak of an isotopic distribution is tabulated. IR spectra were recorded on Bio-Rad FTS-7 spectrometer as Nujol mull between KBr plates. Elemental analyses were performed at the Analytical Laboratory of the Institute of Inorganic Chemistry, University of Göttingen.

Synthesis of LAlMe(OH) (5): Ammonia (40 mL) was condensed onto the suspension of LAlMeCl (**4**; 1.98 g, 4.00 mmol), KOH (>85% KOH, 10−15% H_2O; 0.15 g, 2.33 mmol of KOH (85%), 1.28 mmol of H_2O (15%)), and KH (0.05 g, 1.25 mmol) in toluene (80 mL) at −78 °C with stirring. The mixture was stirred continuously for an additional 1 h at this temperature. The excess ammonia was then allowed to evaporate from the reaction mixture over a period of 4 h. During this time, the mixture was warmed slowly to room temperature. After filtration and subsequent concentration (to 8 mL) in vacuo, the resulting colorless solution was kept at −20 °C for 1 week to isolate colorless crystals of **5** (1.12 g). Isolating the crystals and subsequent partial removal of the solvent from the mother liquor afforded an additional crop of **5** (0.19 g) at −20 °C. Yield 1.31 g (68%). Mp 192 °C. IR (Nujol): $\tilde{\nu}$ = 3728, 1552, 1530, 1373, 1316, 1256, 1189, 1178, 1106, 1056, 1023, 940, 878, 805, 768, 757, 689, 614 cm^{-1}. ^{1}H NMR (300 MHz, C_6D_6): δ = 7.16−7.07 (m, *Ar*), 4.93 (s, 1 H, γ-C*H*), 3.69 (sept, $^3J_{HH}$ = 6.8 Hz, 2 H, C*H*Me$_2$), 3.25 (sept, $^3J_{HH}$ = 6.8 Hz, 2 H, C*H*Me$_2$), 1.57 (s, 6 H, C*Me*), 1.32 (d, $^3J_{HH}$ = 6.8 Hz, 12 H, CH*Me*$_2$), 1.21 (d, $^3J_{HH}$ = 6.8 Hz, 6 H, CH*Me*$_2$), 1.07 (d, $^3J_{HH}$ = 6.8 Hz, 6 H, CH*Me*$_2$), 0.53 (s, 1 H, O*H*), −0.88 (s, 3 H, Al*Me*).

Synthesis of [(LAlMe)(Cp_2ZrMe)](μ-O) (6): Toluene (60 mL) was added to the mixture of **5** (0.48 g, 1.00 mmol) and Cp_2ZrMe_2 (0.25 g, 1.00 mmol). The resulting solution was stirred for 2 h at room temperature, and then continuously for 24 h at 100 °C. The colorless solution was kept at room temperature for 48 h to isolate colorless crystals of **6** (0.51 g). After concentration of the filtrate to 8 mL, the solution was kept at 0 °C for 3 days. An additional crop of **6** (0.15 g) was obtained. Yield 0.66 g (93%). Mp 385 °C (dec). IR (Nujol): $\tilde{\nu}$ = 1518, 1467, 1380, 1316, 1257, 1178, 1101, 1017, 936, 884, 798, 768, 643, 617, 449 cm^{-1}. ^{1}H NMR (300 MHz, $CDCl_3$): δ = 7.25−7.24 (m, *Ar*), 5.31 (s, 10 H, C_5H_5), 5.06 (s, 1 H, γ-C*H*), 3.17 (sept, $^3J_{HH}$ = 6.8 Hz, 2 H, C*H*Me$_2$), 3.15 (sept, $^3J_{HH}$ = 6.8 Hz, 2 H, C*H*Me$_2$), 1.75 (s, 6 H, C*Me*), 1.37 (d, $^3J_{HH}$ = 6.8 Hz, 6 H, CH*Me*$_2$), 1.35 (d, $^3J_{HH}$ = 6.8 Hz, 6 H, CH*Me*$_2$), 1.22 (d, $^3J_{HH}$ = 6.8, 6 H, CH*Me*$_2$), 1.03 (d, $^3J_{HH}$ = 6.8 Hz, 6 H, CH*Me*$_2$), −0.32 (s, 3 H, Zr*Me*), −0.72 (s, 3 H, Al*Me*).

Synthesis of [(LAlMe)(Cp_2ZrCl)](μ-O) (7): In a procedure similar to that for the preparation of **6**, toluene (60 mL) was added to the mixture of **5** (0.48 g, 1.00 mmol) and Cp_2ZrHCl (0.25 g, 1.00 mmol). The resulting colorless solution was kept at room temperature for 48 h to isolate colorless crystals of **7** (0.37 g). After concentration of the filtrate to 10 mL, the solution was kept at 0 °C for 3 days. An additional crop of **7** (0.28 g) was obtained. Yield 0.65 g (89%). Mp 396 °C (dec). IR (Nujol): $\tilde{\nu}$ = 1530, 1466, 1380, 1315, 1254, 1181, 1098, 1022, 943, 860, 797, 778, 759, 725, 657, 617 cm^{-1}. ^{1}H NMR (300 MHz, $CDCl_3$): δ = 7.29−7.21 (m, *Ar*), 5.54 (s, 10 H, C_5H_5), 5.09 (s, 1 H, γ-C*H*), 3.16 (sept, $^3J_{HH}$ = 6.8 Hz, 2 H, C*H*Me$_2$), 3.15 (sept, $^3J_{HH}$ = 6.8 Hz, 2 H, C*H*Me$_2$), 1.78 (s, 6 H, C*Me*), 1.42 (d, $^3J_{HH}$ = 6.8, 6 H, CH*Me*$_2$), 1.36 (d, $^3J_{HH}$ = 6.8 Hz, 6 H, CH*Me*$_2$), 1.24 (d, $^3J_{HH}$ = 6.8 Hz, 6 H, CH*Me*$_2$), 1.02 (d, $^3J_{HH}$ = 6.8 Hz, 6 H, CH*Me*$_2$), −0.66 (s, 3 H, Al*Me*).

X-ray Analysis of 5, 6, and 7. Single crystals of **5**, suitable for X-ray structural analysis, were obtained from toluene solution by maintaining the reaction mixture at −20 °C for 1 week and that of **6** and **7** from toluene solution at room temperature for 48 h. Data for the structure were collected on a STOE IPDS II diffractometer. Intensity measurements were performed on a rapidly cooled crystal in an oil drop.[32] The structure was solved by direct methods (SHELXS-97)[33] and refined with all data by full-matrix least-squares on F^2 (SHELXL-97) (225 parameters). The hydrogen atoms of C−H bonds were placed in idealized positions. Other details of the data collection, structure solution, and refinement are listed in Table 1.

Acknowledgment. This work was supported by the Deutsche Forschungsgemeinschaft, the Fonds der Chemischen Industrie, and the Göttinger Akademie der Wissenschaften. S.S. thanks the Graduierten Kolleg 782 for a fellowship. We thank Dr. Jennifer Kipke, Basell, for molecular weight determinations. Dedicated to Professor Michael Buback on the occasion of his 60th birthday.

Supporting Information Available: X-ray crystallographic data (excluding structure factors) for the structures of **5**, **6**, and **7** reported in this paper. Analysis data (EI-MS and elemental analyses), procedure for ethylene polymerization, determination of (a) TOF value and the polymerization rate, (b) the influence of the concentration of **6** to the TOF value, and (c) the influence of the reaction time of **6** with MAO to the TOF value. This material is available free of charge via the Internet at http://pubs.acs.org.

JA043585W

(32) Clegg, W. *Acta Crystallogr.* **1981**, *A37*, 22−28.
(33) Sheldrick, G. M. *SHELX-97*: *Program for the Solution and Refinement of Crystal Structures*; Universität Göttingen: Göttingen, Germany, 1997.